International Journal of Modern Physics C
Vol. 14, No. 3 (2003) 1–9

World Scientific
www.worldscientific.com

THEORY OF SELF-SIMILAR OSCILLATORY FINITE-TIME SINGULARITIES

D. SORNETTE*,†,‡,¶ and K. IDE*,§,‖

*Institute of Geophysics and Planetary Physics, University of California, Los Angeles, California 90095-1567

†Department of Earth and Space Sciences, UCLA

‡Laboratoire de Physique de la Matière Condensée, CNRS UMR 6622 Université de Nice-Sophia Antipolis, Parc Valrose, 06108 Nice, France

§Department of Earth and Space Sciences, UCLA

¶sornette@moho.ess.ucla.edu

‖kayo@atmos.ucla.edu

Received 2 September 2003
Revised 3 September 2003

A simple two-dimensional system is introduced which suggests a qualitative dynamical relationship between (1) stock market prices in the presence of nonlinear trend-followers and nonlinear value investors, (2) the world human population with a competition between a population-dependent growth rate and a nonlinear dependence on a finite carrying capacity and (3) the failure of materials subjected to a time-varying stress with a competition between positive geometrical feedback on the damage variable and nonlinear healing. Our model keeps three key ingredients (inertia, nonlinear positive and negative feedbacks) that compete to give rise to singularities in finite time decorated by accelerating oscillations.

Keywords: Singularities; population; financial crash; materials rupture; log-periodicity; self-similarity; dynamical systems; spirals.

Singularities play an important role in the physics of phase transitions as well as in signatures of positive feedbacks in dynamical systems, with examples in the Euler equations of inviscid fluids,[1] in vortex collapse of systems of point vortices, in the equations of General Relativity coupled to a mass field leading to the formation of black holes,[2] in models of micro-organisms aggregating to form fruiting bodies,[3] in models of material failure,[4] of earthquakes[5] and of stock market crashes.[6] The continuous scale invariance usually associated with a singularity can be partially broken into a weaker symmetry, called discrete scale invariance (DSI), according to which the self-similarity holds only for integer powers of a specific factor λ (Refs. 7 and 8 and references therein). The observable signature of DSI is the presence of log-periodic oscillations.

Here, we introduce a simple dynamical mechanism for a finite-time singularity with self-similar oscillatory behavior based on the interplay between nonlinear positive feedback and reversal in the inertia.[9] Assuming that the exponents m and n are odd integers, it reads

$$\frac{d^2y_1}{dt^2} = \left(\frac{dy_1}{dt}\right)^m - \gamma y_1^n \,, \tag{1}$$

where y_1 can take negative values. More generally, we can account for noninteger and/or non-odd values of m and n by introducing absolute values. This leads to the following general extension of Eq. (1), represented as a dynamical system:

$$\begin{aligned} \frac{dy_1}{dt} &= y_2 \,, \\ \frac{dy_2}{dt} &= y_2|y_2|^{m-1} - \gamma y_1|y_1|^{n-1} \,. \end{aligned} \tag{2}$$

Our analysis of Eq. (2) may suggest a more fundamental understanding of the observed interplay between accelerating growth and accelerating oscillations previously documented in speculative bubbles preceding large crashes[6,10] (see Refs. 11 and 12 for a critical exchange discussing the pros and cons of this controversial theory and references therein), the world human population,[13,14] and time-to-failure analysis of material rupture[4] (and references therein).

Stock market price dynamics: The heterogeneous behavior of agents has recently been shown to be a crucial ingredient to account for the complexity of financial time series (see Ref. 15 and references therein). Typically, "value investors" track the fundamental price p_f of a given stock placing investment orders of (algebraic) size $\Omega_{\rm value}(t)$ while "technical analysts" use trend following strategies to place investment orders of size $\Omega_{\rm tech}(t)$. The balance between supply and demand is assumed to determine the price variation from $p(t)$ to $p(t+\delta t)$ over the time interval δt according to $\ln p(t+\delta t) - \ln p(t) = 1/D[\Omega_{\rm value}(t) + \Omega_{\rm tech}(t)]$,[16–18] where $D > 0$ is a market depth. We postulate the nonlinear dependence $\Omega_{\rm value}(t) = -c \ln[p(t)/p_f]|\ln[p(t)/p_f]|^{n-1}$, where $n > 1$ and $c > 0$ is a constant. The case $n = 1$ retrieves an ingredient of previous models.[16,19] According to textbook economics, p_f is determined by the discounted expected future dividends whose estimation is very sensitive to the forecast of their growth rate and of the interest rate, leading to large uncertainties in p_f. As a consequence, a trader trying to track fundamental value has no incentive to react when she feels that the deviation is small since this deviation is more or less within the noise. Only when the departure of price from fundamental value becomes relatively large will the trader act. The exponent $n > 1$ precisely accounts for this effect. The second class of investors follow strategies that are positively related to past price moves. This can be captured by the following contribution to the order size: $\Omega_{\rm tech}(t) = a_1[\ln p(t) - \ln p(t-\delta t)] + a_2[\ln p(t) - \ln p(t-\delta t)]|\ln p(t) - \ln p(t-\delta t)|^{m-1}$ with $a_1 > 0$ and $a_2 > 0$. The choice $m > 1$ means that trend-following strategies

tend to under-react for small price changes and over-react for large ones. We stress that the nonlinear reactions of fundamentalists ($n > 1$) and of chartists ($m > 1$), which allow for overshooting, is the opposite of usual assumptions in similar financial models,[20,21] where the possibility of overshooting is not investigated.

Posing $y_1(t) = \ln[p(t)/p_f]$, we expand the equation of balance between supply and demand as a Taylor series in powers of δt and get

$$(\delta t)^2 \frac{d^2 y_1}{dt^2} = -\left[1 - \frac{a_1}{D}\right] \delta t \frac{dy_1}{dt} + \frac{a_2 (\delta t)^m}{D} \frac{dy_1}{dt} \left|\frac{dy_1}{dt}\right|^{m-1} - \frac{c}{D} y_1(t) |y_1(t)|^{n-1} + \mathcal{O}[(\delta t)^3] \,,$$

where $\mathcal{O}[(\delta t)^3]$ represents a term of the order of $(\delta t)^3$. This equation is a generalization of the model of Pandey and Stauffer,[22] by allowing nonlinear positive feedback $m > 1$ of the trend-following strategies. The theory becomes critical when the "mass" term vanishes, i.e., when $a_1 = D$. Rescaling t and y_1 by α and posing $y_t = dy_1/dt$ and $\gamma = \alpha^{-(n+1)} c/D(\delta t)^2$ where $\alpha \equiv a_2 (\delta t)^{m-2}/D$, we obtain Eq. (2).

Population dynamics: The logistic equation corrects Malthus' exponential growth model by assuming that the population $p(t)$ cannot grow beyond the earth carrying capacity K: $dp/dt = \sigma_0 p(t)[K - p(t)]$ where σ_0 controls the amplitude of the nonlinear saturation term (see Ref. 23 and references therein). However, it is now understood that K is not a constant but increases with $p(t)$ due to technological progress such as the use of tools and fire, the development of agriculture, the use of fossil fuels, fertilizers etc. as well an expansion into new habitats and the removal of limiting factors by the development of vaccines, pesticides, antibiotics. If $K(t)$ grows faster than $p(t)$, then $p(t)$ explodes to infinity after a finite time creating a singularity due to the corresponding growth of the growth rate $\sigma \equiv d \ln p/dt$, leading to $d\sigma/dt \propto \sigma^2$.[14] We now generalize it by assuming a nonlinear saturation: $d\sigma/dt = \alpha \sigma |\sigma|^{m-1} - \gamma \ln(p/K_\infty) |\ln(p/K_\infty)|^{n-1}$ where α and $\gamma > 0$ measure the effect of feedback and reversal. Apart from the absolute value, the first term in the r.h.s. is the previous nonlinear growth of the growth rate. The novel second term favors a restoration of the population $p(t)$ to the asymptotic carrying capacity K_∞. The effective cumulative growth rate $\ln(p/K_\infty)$ is the natural variable to describe the attraction to K_∞. The nonlinear restoring exponent $n > 1$ captures the many nonlinear (often quasi-threshold) feedback mechanisms acting on population dynamics. Defining variables $(y_1, y_2) = (\alpha \ln(p/K_\infty), \sigma)$ and rescaling t by α lead to Eq. (2).

Rupture of materials with competing damage and healing: A standard model of damage rupture[24] consists in a rod subjected to uniaxial tension by a constant applied axial force P. The undamaged cross section $A(t)$ of the rod is assumed to be a function of time but is independent of the axial coordinate. The considered viscous deformation is assumed to be isochoric: $A_0 L_0 = A(t) L(t) =$ constant at all times, where $L(t)$ is the length of the rod. The creep strain rate

$d\epsilon_c/dt = (1/L)(dL/dt) = -(1/A)(dA/dt)$ is assumed to follow Norton's law: $d\epsilon_c/dt = C\sigma^\mu$ where $\sigma = P/A$ is the rod cross section with $C > 0$ and $\mu > 0$ Eliminating $d\epsilon_c/dt$ leads to $A^{\mu-1}dA/dt = -CP^\mu$, and hence $d\sigma/dt = C\sigma^{\mu+1}$. Physically, this results from a geometrical feedback of the undamaged area on the stress and vice-versa.

We generalize this model by adding healing as well as a strain-dependent loading: $d\sigma/dt = \alpha\sigma|\sigma|^{m-1} - \gamma\epsilon_c|\epsilon_c|^{n-1}$. The first term in the right-hand-side is identical to previous geometrical positive feedback for $m = \mu - 1$. We relax this correspondence and allow $m > 1$ to be arbitrary. The addition of the second term introduces the physical ingredient that damage can be reversible. Large deformations can enhance healing which increases the undamaged area and thus decrease the effective stress within the material. The model is completed by using again Norton's law but with exponent m': $d\epsilon_c/dt = C\sigma^{m'}$. Incorporating the constant C in a redefinition of time $Ct \to t$ (with suitable redefinitions of the coefficients $\alpha/C \to \alpha$ and $\gamma/C \to \gamma$), taking $m' = 1$ and posing $(y_1, y_2) = (\epsilon_c, \sigma)$, we retrieve Eq. (2).

Analysis of the dynamical system Eq. (2) for $n > 1$ and $m > 1$ with $\gamma \geq 0$: When only the reversal term is present (i.e. the term $y_2|y_2|^{m-1}$ is absent), Eq. (2) describe a nonlinear oscillator with conserved Hamiltonian $H(\mathbf{y}; n, \gamma) \equiv \gamma/n + 1(y_1^2)^{(n+1)/2} + 1/2y_2^2$. A trajectory is periodic along a constant H with period

$$T(H; n, \gamma) = C(n)\gamma^{-1/(n+1)}H^{1-n/2(n+1)}\,, \tag{3}$$

where $C(n)$ is a positive number that can be explicitly calculated.[9]

When only the positive feedback is present (i.e. $\gamma = 0$), Eq. (2) leads to a finite-time singularity. The solution $\mathbf{y}(t; \mathbf{y}_0, t_0)$ with initial condition $\mathbf{y}_0 = (y_{10}, y_{20})$ at time t_0 is:

$$\mathbf{y}_1(t; \mathbf{y}_0, t_0) - y_{10} = \mathrm{sign}[y_{20}]\frac{(m-1)^{\hat{m}}}{2-m} \times [(t_c(y_{20}) - t)^{\hat{m}} - (t_c(y_{20}) - t_0)^{\hat{m}}] \quad \text{for } m \neq 2\,, \tag{4}$$

where $\hat{m} = (m-2)/(m-1)$. For $m = 2$, $y_1(t; \mathbf{y}_0, t_0) - y_{10} = \mathrm{sign}[y_{20}]\log((t_c - t_0)/t_c(y_{20}) - t)$.

$$y_2(t; \mathbf{y}_0, t_0) = \mathrm{sign}[y_{20}](m-1)^{-1/m-1}(t_c(y_{20}) - t)^{-1/(m-1)}\,, \tag{5}$$

where the $t_c(y_{20}) - t_0 = 1/(m-1)|y_{20}|^{1-m}$ depends only on y_{20}. As $t \to t_c(y_{20})$, y_2 becomes either $+\infty$ or $-\infty$ depending on the sign of y_{20} for any $m > 1$. For $1 < m \leq 2$, it is easy to show that $|y_1|$ also becomes infinity as $t \to t_c(y_{20})$. In contrast, for $m > 2$, y_1 remains finite. We thus think that $m > 2$ is the relevant physical regime for the financial, population and rupture problems discussed above. From here on, our analysis focuses on $n > 1$ and $m > 2$.

Putting the nonlinear oscillation and positive feedback terms together, the dynamics of (2) is characterized in Fig. 1. The two special intertwined trajectories along b^+ (solid line) and b^- (dashed line) connect the origin (0, 0) to $(+\infty, +\infty)$

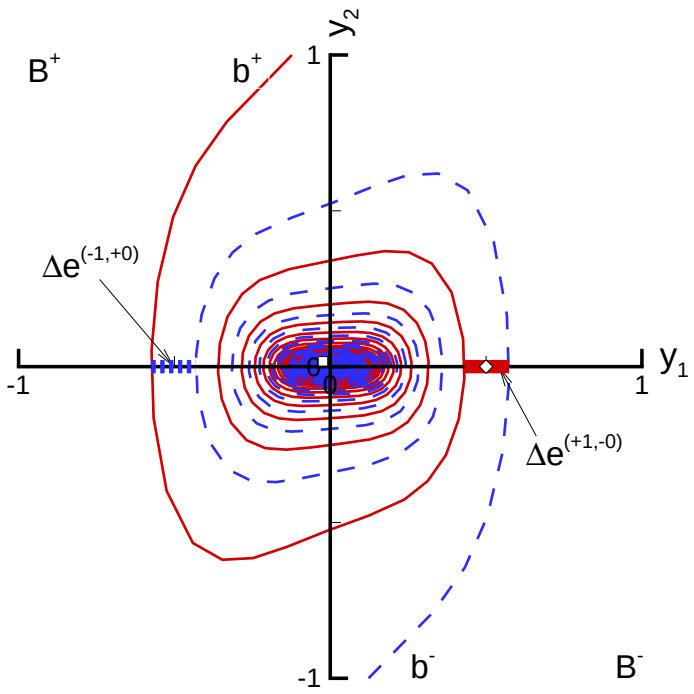

Fig. 1. Geometry of the boundaries b^+ and b^- as well as the basins B^+ and B^- for $(n, m) = (3, 2.5)$ and $\gamma = 10$ in phase space: the exit segments $\triangle e^{(+1,-0)} \in B^+$ and $\triangle e^{(-1,+0)} \in B^-$ are thick solid and dashed lines respectively on the y_1-axis; the squares and diamonds are the initial condition and exit point of the trajectory in Fig. 2.

and $(-\infty, -\infty)$, respectively, and hence divide the phase space $\mathbf{y} \equiv (y_1, y_2)$ into two distinct basins B^+ and B^-. The basin B^+ (resp. B^-) corresponds to a finite-time singularity $\mathbf{y}_c(\mathbf{y}_0)$ with $y_{2c}(\mathbf{y}_0) = +\infty$ (resp. $y_{2c}(\mathbf{y}_0) = -\infty$) but finite $y_{1c}(\mathbf{y}_0)$ at the critical time $t_c(\mathbf{y}_0)$.

Starting from $\mathbf{y}_0$ in B^+ close to the origin at t_0, a trajectory $\mathbf{y}(t; \mathbf{y}_0, t_0)$ spirals out with clockwise rotation and we count a turn each time it crosses the y_1-axis, i.e. y_1 changes its direction of motion ($dy_1/dt = 0$). Deep in the spiral structure, $\mathbf{y}(t; \mathbf{y}_0, t_0)$ follows approximately the orbit of constant Hamiltonian H defined by the nonlinear oscillator but fails to close on itself because H is no longer conserved due to the positive feedback:

$$\frac{d}{dt} H(\mathbf{y}; n, m, \gamma) = |y_2|^{m+1} \geq 0\,. \tag{6}$$

This slowly growing nonlinear oscillator defines the first dynamical regime.

Any trajectory starting in the first dynamical regime must eventually cross-over to the second one associated with a route to the singularity without any further oscillation. In the second dynamical regime, y_2 diverges (and therefore dy_2/dt also diverges) while y_1 remains finite on the approach to $t_c(\mathbf{y}_0)$. As a consequence, the reversal term $\gamma y_1 |y_1|^{n-1}$ in dy_2/dt Eq. (2) becomes negligible close to $t_c(\mathbf{y}_0)$ and

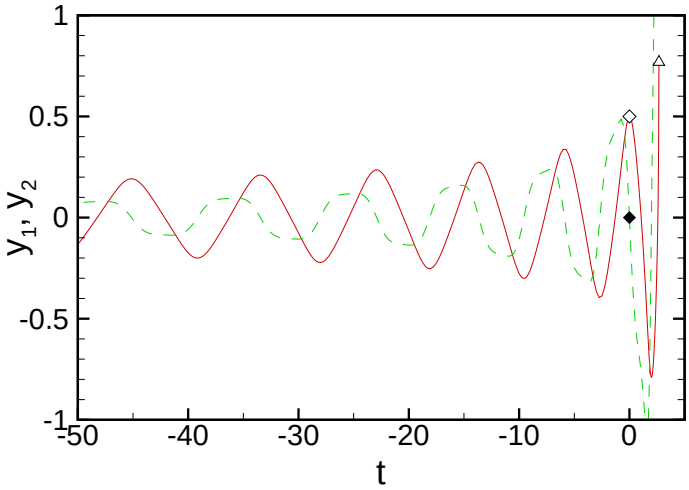

Fig. 2. A trajectory in B^+ starting from initial condition $(-2.32878 \times 10^{-2}, 1.71083 \times 10^{-2})$ at $t = -500$, going through the exit point (0.5, 0) at $t = 0$, to the critical point $(0.768899, +\infty)$ at $t_c = 2.67284$: Solid and dashed lines correspond to y_1 and y_2, respectively; diamond and triangle are the point in the exit segment $\triangle e^{(+1,-0)}$, and the critical point along the trajectory with open and filled symbols corresponding to y_1 and y_2.

Eq. (4) is the asymptotic solution of Eq. (2). Figure 2 shows a typical time series of a $\mathbf{y}(t; \mathbf{y}_0, t_0)$ starting from $\mathbf{y}_0$ near the origin.

In the basin B^+, the transition from the first to second dynamical regime occurs at the exit segment $\triangle e^{(+1,-0)}$ on the positive y_1-axis (Fig. 1) whose right and left end-points according to the forward direction of the flow are defined by the boundaries b^+ and b^-, respectively. In forward time, $\triangle e^{(+1,-0)}$ fans out rapidly over $y_1 \in (-\infty, \infty)$ as it reaches a singularity with $y_2 \to +\infty$ in the second dynamical regime. Note that $|y_1|$ can reach ∞ if and only if $\mathbf{y}_0$ is at an end point of $\triangle e^{(+1,-0)}$, i.e. on either b^+ or b^-. Similar results hold for the exit segment $\triangle e^{(-1,+0)}$ in B^- but with $y_2 \to -\infty$. In backward time, $\triangle e^{(+1,-0)}$ and $\triangle e^{(-1,+0)}$ swirl into the origin while making countable infinite many turns.

The first dynamical regime exhibits remarkable scaling properties that we quantify by the dependence on the initial condition $\mathbf{y}_0 = (y_{10}, 0)$ on the y_1-axis of the following quantities: the number ($N_{\rm turn}$) of turns before reaching the singularity, the exit time (t_e) to reach the exit segment into the second dynamical regime, the time interval (Δt_e) and the increment (Δy_1) in the amplitude of y_1 over one turn. Figure 3 shows log-log plots of the scaling properties measured at the kth backward intersection of b^+ with the y_1-axis starting from $k = 0$ at the out-most intersection (the left end-point of $\triangle e^{(-1,+0)}$ in Fig. 1).

The log–log dependences shown in Fig. 3 qualify power laws defined by

$$N_{\rm turn} \sim y_{10}^{-a}\,, \quad \text{where } a > 0\,,$$
$$t_e \sim y_{10}^{-b}\,, \quad \text{where } b > 0\,, \tag{7}$$

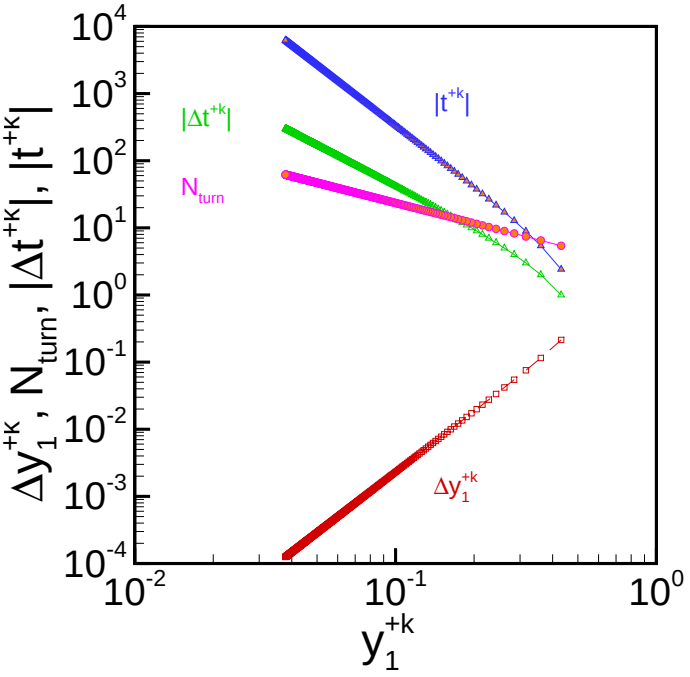

Fig. 3. Scaling laws associated with the self-similar properties of the nonlinear oscillatory regime as a function of initial conditions at turn points for $(n, m) = (3, 2.5)$ and $\gamma = 10$.

$$\Delta y_{10} \sim y_{10}^{c}\,, \qquad \text{where } c > 0\,, \tag{8}$$

$$\Delta t_e \sim y_{10}^{-d}\,, \qquad \text{where } d > 0\,. \tag{9}$$

Eliminating y_{10} between (7) and (9) gives $\Delta t_e \sim t_e^{d/b}$. Since Δt_e is nothing but the difference $\Delta t_e = t_e(N_{\rm turn}+1) - t_e(N_{\rm turn})$, this gives the discrete difference equation $t_e(N_{\rm turn}+\Delta N_{\rm turn}) - t_e(N_{\rm turn})/\Delta N_{\rm turn} \propto t_e^{d/b}$, where $\Delta N_{\rm turn} = N_{\rm turn}+1-N_{\rm turn} = 1$. This provides a discrete difference representation of the derivative $dt_e/dN_{\rm turn}$ which can be integrated formally to give $N_{\rm turn} \sim t_e^{1-d/b}$, which is valid for $d < b$. Comparing with the relation between $N_{\rm turn}$ and t_e obtained by eliminating y_{10} between Eq. (7) and Eq. (7), i.e. $N_{\rm turn} \sim t_e^{a/b}$, we get the scaling relation

$$a = b - d\,. \tag{10}$$

Since $a > 0$, the condition $d < b$ is automatically verified.

Similarly, $\Delta y_{10} = y_{10}(N_{\rm turn}+1) - y_{10}(N_{\rm turn}) \propto y_{10}^{c}$ according to definition (8). This gives the differential equation $dy_{10}/dN_{\rm turn} \sim y_{10}^{c}$, whose solution is $N_{\rm turn} \sim 1/y_{10}^{c-1}$, valid for $c > 1$. Comparing with the definition Eq. (7), we get the second scaling relation

$$a = c - 1\,. \tag{11}$$

Since $a > 0$, the condition $c > 1$ is automatically satisfied.

Deep in the spiral structure shown in Fig. 1, the time Δt_e needed to make one full (almost closed) rotation is very close to the period $T(H)$ without the positive feedback term. This is essentially an adiabatic approximation in which the Hamiltonian H and the period $T(H)$ are assumed to vary sufficiently slowly. Putting together Eq. (3) and the fact that the amplitude of the initial value y_{10} is proportional to $H^{1/n+1}$, we get $\Delta t_e \sim |y_{10}|^{(1-n)/2}$, which, by comparison with Eq. (9), gives

$$d = \frac{n-1}{2}\,. \tag{12}$$

The last equation is provided by dT/dt, expressed as $dT/dt = (dT/dH) \times (dH/dt)$, where dT/dH is obtained by differentiating Eq. (3) and dH/dt is given by Eq. (6). Estimating dT/dH from Eq. (3) is consistent with the above approximation in which a full rotation along the spiral takes the same time as the corresponding closed orbit in absence of the positive feedback term. Expressing dH/dt using Eq. (6) involves another approximation, which is similar in spirit to a mean-field approximation corresponding to average out the effect of the positive feedback term over one full rotation. We replace dT/dt by $d\Delta t_e/dt_e$ and obtain $d\Delta t_e/dt_e \sim H^{-3n+1/2(n+1)}|y_2|^{m+1} \sim \Delta t_e^{3n+1/n-1}|y_{10}|^{(n+1)(m+1)/2}$, where the dependence in Δt_e is derived by replacing H by its dependence as a function of T (by inverting $T(H)$) and by identifying T and Δt_c. We have also used $|y_2| \sim |y_{10}|^{(n+1)/2}$. Taking the derivative of $\Delta t_e \sim t_e^{d/b}$ with respect to t_e provides another estimation of $d\Delta t_e/dt_e$, and replacing Δt_e in the above equation by its dependence as a function of y_{10} as defined by Eq. (9) gives finally:

$$a = \frac{1}{2}(n+1)(m+1) - \frac{1}{2}(3n+1)\,. \tag{13}$$

We find very good agreement between the theoretical predictions Eqs. (10), (11), (12), (13) with an estimation obtained from the direct numerical integration of the dynamical equations.[9] We have also verified the independence of the exponents a, b, c, d with respect to the amplitude γ of the reversal term.[9] We shall report elsewhere on tests of this theory on financial and rupture data.

In the oscillatory regime, the growth of the amplitude $A_{y_1}(t)$ of $y_1(t)$ follows a power law similar to Eq. (4), namely $A_{y_1}(t) = B/(t^* - t)^{1/b}$, which is nothing but the inverse of Eq. (7) (see Ref. 9 for a detailed derivation). The time t^* is a constant of integration, which can be interpreted as an *apparent* or "ghost" critical time. t^* has no reason to be equal to t_e, in particular since the extrapolation of $A_{y_1}(t) = B/(t^*-t)^{1/b}$ too close to t^* would predict a divergence of $y_1(t)$. The dynamical origin of the difference between t^* and t_c comes from the fact that t^* is determined by the oscillatory regime while t_c is the sum of two contributions, one from the oscillatory regime and the other from the singular regime. This prediction is verified accurately from our direct numerical integration of the equations of motion.[9]

Combining Eq. (9) with this solution for $A_{y_1}(t)$ gives the time dependence of the local period Δt_e of the oscillation in the oscillatory regime as $\Delta t_e = t_{k+1} - t_k \sim$

$(t^* - t_k)^{d/b}$, where k counts the number of turns (or oscillations). This result generalizes the log-periodic oscillation associated with discrete scale invariance (DSI) mentioned in the introduction, characterized by $t_{k+1} - t_k \sim 1/\lambda^k$ (where $\lambda > 1$ is a preferred scaling ratio of DSI). This exact log-periodicity is recovered in the formal limit $d/b \to 1^-$ (corresponding to $(n \to \infty, m \to 2)$ leading to $y_1 \sim \ln(t_c - t)$, $y_2 \sim 1/(t_c - t)$ and $a \to 1$, $b \to \infty$, $c \to 2$, $d \to \infty$ The dynamical system Eq. (2) provides a mechanism for accelerating oscillations with, in addition, a finite number of them due to the cross-over to the nonoscillatory regime.

Acknowledgments

This work was partially supported by ONR N00014-99-1-0020 (KI) and by NSF-DMR99-71475 and the James S. Mc Donnell Foundation 21st century scientist award/studying complex system (DS).

References

1. A. Pumir and E. D. Siggia, *Phys. Rev. A* **45**, R5351 (1992).
2. M. W. Choptuik, *Prog. Theor. Phys. Suppl.* **136**, 353 (1999).
3. M. Rascle and C. Ziti, *J. Math. Biol.* **33**, 388 (1995).
4. A. Johansen and D. Sornette, *Eur. Phys. J. B* **18**, 163 (2000).
5. A. Johansen, H. Saleur, and D. Sornette, *Eur. Phys. J. B* **15**, 551 (2000).
6. A. Johansen, D. Sornette, and O. Ledoit, *J. Risk* **1**, 5 (1999).
7. D. Sornette, *Phys. Rep.* **297**, 239 (1998).
8. D. Sornette, *Critical Phenomena in Natural Sciences* (Springer Series in Synergetics, Heidelberg, 2000).
9. K. Ide and D. Sornette, *Physica A* **307**, 63 (2002).
10. A. Johansen and D. Sornette, *Eur. Phys. J. B* **17**, 319 (2000).
11. J. A. Feigenbaum, *Quant. Fin.* **1**, 346 (2001).
12. D. Sornette and A. Johansen, *Quant. Fin.* **1**, 452 (2001).
13. S. P. Kapitza, *Uspekhi Fizichskikh Nauk* **166**, 63 (1996).
14. A. Johansen and D. Sornette, *Physica A* **294**, 465 (2001).
15. T. Lux and M. Marchesi, *Nature* **297**, 498 (1999).
16. J. D. Farmer, preprint adap-org/9812005.
17. B. Rosenow, *Int. J. Mod. Phys. C* **13**, 419 (2002).
18. F. Lillo, J. D. Farmer, and R. N. Mantegna, preprint at cond-mat/0207428.
19. J.-P. Bouchaud and R. Cont, *Eur. Phys. J. B* **6**, 543 (1998).
20. C. Chiarella, *Annals Oper. Res.* **37**, 101 (1992).
21. P. De Grauwe, H. Dewachter, and M. Embrechts, *Exchange Rate Theory, Chaotic Models of Foreign Exchange Markets* (Blackwell, Oxford, UK, 1993).
22. R. B. Pandey and D. Stauffer, *Int. J. Theor. Appl. Fin.* **3**, 479 (2000); C. Schulze, *Int. J. Mod. Phys. C* **13**, 551 (2002); A. Proykova, L. Roussenova, and D. Stauffer, paper for APFA 3 (London Dec.2001); I. Chang, D. Stauffer, and R. B. Pandey, *Int. J. Theor. Appl. Finance* 5(b), (2002).
23. J. E. Cohen, *Science* **269**, 341 (1995).
24. D. Krajcinovic, *Damage Mechanics* (North-Holland, Elsevier, Amsterdam, 1996).